P8.3

STATISTICAL RELATIONSHIPS BETWEEN SATELLITE-DERIVED MESOSCALE ATMOSPHERIC MOTION VECTORS, RAWINSONDES, AND NOAA WIND PROFILER NETWORK OBSERVATIONS

Kristopher Bedka [(1)] *, Wayne F. Feltz [(1)], John R. Mecikalski [(2)], Ralph A. Petersen [(1)], and Christopher S. Velden [(1)]

[(1)] Cooperative Institute for Meteorological Satellite Studies, University of Wisconsin–Madison
[(2)] Atmospheric Sciences Department, University of Alabama in Huntsville

1. INTRODUCTION

GOES satellite-derived atmospheric motion vectors (AMVs) have recently been shown to capture detailed mesoscale flow structure in the vicinity of convective storms, which can be used to compute convective cloud-top growth rates (Bedka and Mecikalski 2005, BM05 hereafter). Using the UW-CIMSS satellite AMV algorithm (Velden et al. 1997, 1998) to help diagnose a severe thunderstorm event over the U.S. Southern Plains, BM05 show that a modified mesoscale AMV processing methodology increases the number of vectors by a factor of 20 over typical operational methods. An example of AMVs from this event is shown in Figure 1. Although these mesoscale AMVs are effective in identifying cumulus cloud motions, little published information is available on the quality of these mesoscale motion vectors.

The focus of this presentation is to evaluate specially-processed GOES-12 mesoscale AMVs using two established ground-based in situ observing systems: the NOAA Wind Profiler network and rawinsondes (i.e. "sondes"). Wind observations are matched in time/space with mesoscale AMVs over the U.S. Department of Energy (DOE) Atmospheric Radiation Measurement (ARM) program Southern Great Plains (SGP) Central Facility at Lamont, OK. Root-mean-square (RMS) difference and bias statistics are computed. Routine operational GOES-12 AMVs from NOAA/NESDIS are also incorporated into this analysis to compare and contrast the RMS and bias statistics between operational and mesoscale AMVs.

Establishing the observation "error" characteristics of mesoscale AMVs can lead to an improved utilization of these vectors in any application where detailed knowledge of atmospheric flow is required at high temporal resolution. For example, these AMVs are currently being produced at CIMSS and used as input to an experimental convective storm initiation nowcast algorithm (Mecikalski and Bedka 2005). The AMVs can also be interpolated to aviation flight levels for shear-induced turbulence identification and for more efficient aircraft route planning to avoid (benefit) from regions with strong head-winds (tail-winds). In addition, assimilation of these high-density AMVs into mesoscale NWP models is another potential application.

* Corresponding Author: Kristopher M. Bedka, Cooperative Institute for Meteorological Satellite Studies, UW-Madison, 1225 West Dayton Street, Madison, WI 53706. Email: krisb@ssec.wisc.edu

2. METHODOLOGY AND DATASETS

2.1. Mesoscale AMV Processing Methods

The methodology for deriving mesoscale AMVs is explained in detail in BM05, but is summarized below. A 3-image sequence of 15-min temporal resolution GOES-12 1-km visible (VIS), 4-km 10.7-μm "infrared window" (IR), and 4-km 6.5-μm water vapor (WV) band data is used as input to the UW-CIMSS AMV processing algorithm. Targets are identified in boxes of adjustable size within the middle image of this sequence and are tracked both forward and backward in time using cross-correlation based feature matching. Suitable targets represent well-defined cloud features (VIS, IR), coherent cloud edges (VIS, IR), or brightness temperature (T_B) gradients in the WV channel. Two "sub-vectors" are computed and are then averaged to arrive at a final vector motion for a given target.

The next step is to obtain an estimate of the height for each AMV. This is accomplished by a hierarchical scheme (Velden et al. 1998) that selects one of several available IR-based techniques: the "IR window" technique (Schreiner et al. 1993); the CO_2-slicing algorithm (Menzel et al. 1983); or the H_2O-intercept method (Szejwach 1982; Nieman et al. 1997).

The AMVs are then post-processed using objective quality control (QC) routines. These routines check the temporal and spatial coherence of the AMVs [the "quality indicator" (QI) technique, Holmlund 1998] and the fit of each individual vector to an objective analysis of the wind field ["recursive filter" (RF) analysis, Hayden and Purser 1995]. While an NWP model guess is used as a background for the objective analysis, the required fit of the final AMV field to the model first guess is reduced in mesoscale AMV processing because the model often cannot accurately resolve and represent the complex flow associated with (and induced by) convective clouds on the meso-γ (sub-grid) and meso-β scales due to grid resolution limitations.

Additional differences between operational and mesoscale AMV processing are described below. The principle goals of these adjustments are to increase the number of targets for subsequent tracking, and to relax the quality control constraints primarily developed to satisfy a coherent AMV field for larger-scale flow regimes. Both of these processing strategy modifications serve to increase the density and detail of the resulting AMV field to better depict mesoscale flow regimes.

- The size of the AMV targeting box is reduced from the default size of 15 x 15 to 5 x 5 pixels (~1-km (VIS) and ~4-km (IR) resolution per pixel).

- VIS targets are tracked through the entire depth of the troposphere and lower stratosphere (1000-100 hPa); this differs from operational processing, where targets are only identified in the lower- to mid-troposphere (1000-600 hPa).

- The maximum IR target T_B is increased from 250 to 285 K in order to allow tracking of lower-tropospheric cumulus clouds in warm boundary layers.

- The impact of the internal quality control on the resulting AMV field is greatly down-weighted through a reduction of the minimum required QI (50 vs. 60 (operational)) and RF (.01 vs. .50 (operational)) analysis score thresholds.

- Gross error checks that penalize directional and speed variations from the background guess field (typically 90° and 10 ms^{-1}) are turned off to further minimize the impact of the first-guess on the final mesoscale AMV field.

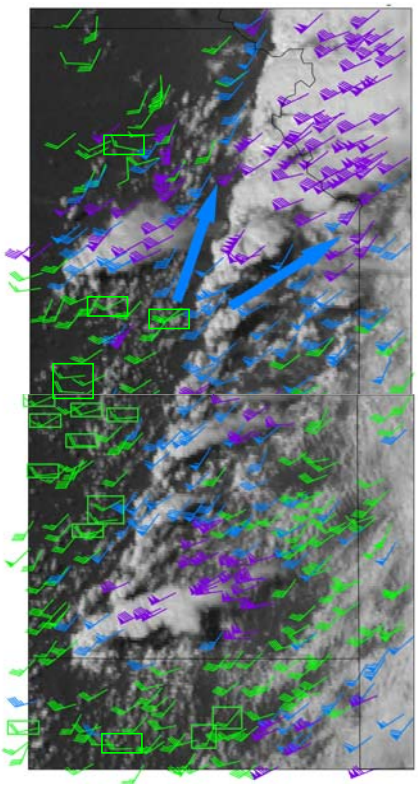

Figure 1: GOES-12 mesoscale AMVs superimposed on VIS imagery within and near developing convection over Eastern KS at 2000 UTC on 4 May 2003. Green barbs represent AMVs within the 1000-700 hPa layer; blue barbs within the 700-400 hPa layer, purple barbs within the 400-100 hPa layer. Green barbs outlined by boxes illustrate convergent flow at levels below 900 hPa. Large blue arrows illustrate mid-level diffluent flow.

It is important to note here that, like any other observing system, satellite-derived AMVs are inherently unable to perfectly depict the "true" flow at any given point in the troposphere, even if the AMV target characteristics (horizontal dimension, cloud-top opacity/emissivity) and their behavior in time are optimal. The underlying assumptions of satellite-derived motion estimation are that features move within an short-term image sequence at a constant height level, with speeds equal to the true atmospheric flow. The first assumption can be violated in convective cloud situations, especially if the image sequence separation time is large compared to the vertical motions. The latter assumption is difficult to prove with the current generation observing systems as no "perfect" wind measurement device exists. Finally, vertical momentum transports occurring in "clear-air" (i.e. cloud-free regions) induced by cumulus cloud dynamics and phenomena such as boundary layer eddies and gravity wave circulations cannot be directly measured from satellites. These transports can alter the actual flow as measured by in situ rawinsondes or Wind Profilers.

The following bullets provide a brief summary of the target characteristics, time evolution behavior, and NWP first guess characteristics that would lead to an optimal AMV flow estimate using geostationary imagery. An appreciable portion of the AMV versus sonde and Profiler differences in this study are likely related to deviations from these guidelines, with errors associated with height assignment being the largest contributor. It should also be stated that rawinsonde/Profiler measurement errors and matching collocation induced errors also contribute to the differences shown in Section 3.

Optimal AMV Target Characteristics:

- Steady-state cloud features neither growing nor decaying in the vertical, with sharp, coherent edges.

- Cloud and WV targets represent a single/shallow tropospheric level/layer.

- A VIS or IR target should fill an entire 4 km IR pixel, with an opaque cloud-top and an emissivity near 1, for the best application of the IR-based height assignment techniques.

- WV tracking targets representing a shallow layer of concentrated WV within the middle to upper troposphere (Rao et al. 2002), and exhibiting sharp horizontal gradients.

- Distinct appearance of target relative to the Earth surface (i.e. target much colder than surface, no surface snow or ice cover).

- Targets within ~60° of the satellite nadir point. Degredation can be expected outside of this radius towards the limbs of the satellite view.

Optimal AMV Target Tracking and Evolution Behavior

- Tracking image separation: 5 mins for VIS/IR and 30 mins for WV.
- Coherency in the shape and motion of the target over the tracking interval (i.e. non-accelerating, subvector 1 speed equal to subvector 2 speed).
- Image-to-image geo-referenced co-registration accurate to within ~1 pixel.

Optimal NWP Background Guess Characteristics

- For the applications discussed in this study, mesoscale NWP model analyses with high spatial and vertical resolution to obtain accurate temperature profiles for use in AMV height assignments.

2.2. NOAA Wind Profiler and Rawinsonde Data

Six-minute resolution data from the NOAA Wind Profiler site at Lamont, OK is utilized within this study. As the satellite AMV heights are assigned in pressure space, the sampling levels of the Profiler are converted from altitude (in meters) to pressure (in millibars) using the initial pressure/height analysis profile from the operational Rapid Update Cycle 20-km resolution model run (RUC-20, Benjamin et al. 2002). As a 3-image sequence of GOES-12 data is used to compute AMVs over a 30-min time window, six 6-minute wind profiles are averaged together (centered in time on the middle GOES image) to obtain a set of wind observations that is reasonable and "fair" to compare with GOES AMVs. Only high-quality Profiler data, which pass all QC checks, are used here.

Rawinsondes launched from the DOE ARM SGP Central Facility at Lamont, OK are also employed for AMV evaluation purposes in this study. Specifically, Vaisala RS-92 GPS-tracked, quality controlled, wind measurements are co-located with and compared to the GOES AMVs and Wind Profiler data. There are four sonde launches per day at the Lamont site, occurring at approximately 0530, 1130, 1730, and 2330 UTC. In addition, supplemental sonde launches are also included, which vary in launch time to coincide with polar orbiting satellite (AQUA) overpasses. In total, data from 742 rawinsondes are used for comparison.

2.3. Dataset Collocation Methodology

The period of 04/11/05 to 10/01/05 has been evaluated to date. Plans are to expand this study to a period of one year, such that a statistically significant sample size of collocated data, representing a comprehensive set of mesoscale atmospheric conditions, is accumulated.

Two types of comparisons will be shown in Section 3. One will include spatially and temporally collocated Wind Profiler and sonde information at each Profiler sampling level. This comparison is done to demonstrate the relative accuracy and consistency of the 6-min Wind Profiler observations. As each sonde reports data from thousands of vertical levels, a large number of collocations exist, which allows for a robust analysis of the difference characteristics between these two instruments. Once these characteristics have been established, a second comparison is performed which includes GOES-12 operational and mesoscale AMVs, Profiler, and sonde data.

The time and location of the rawinsonde observations at each sonde level is compared to the time stamp of a Wind Profiler observation. Profiler observations within +/- 3-mins of the sonde observation and 2-hPa in the vertical are considered matches. As the sonde ascends with time, a Profiler observation temporally closest to the sonde observation is selected for comparison. Thus for a 1-hour sonde flight, as many as 11 different Wind Profiler profiles are directly compared to the sonde data. A 25-km spatial match criteria is imposed such that the Wind Profiler and sonde are both sampling a homogeneous atmospheric state. It is important to note that this criterion essentially imposes a bias within this comparison toward lower wind speeds, as a high wind situation would likely advect the balloon outside of the 25-km-radius vertical column surrounding the Wind Profiler. Future work will examine the impact of expanding this radial distance match threshold.

The second comparison focuses on the quality of the GOES-12 AMV estimates. AMVs within 25 km of the Lamont, OK Wind Profiler site are collected each time the UW-CIMSS algorithm is executed (every 15-mins during both the day and night). A 25-km radial distance threshold is also applied to the sonde data, similar to the comparison described above. Profiler and sonde data are matched if they are within 2 hPa of one another. An AMV is then matched to these datasets if its height is within 10 hPa of the Profiler/sonde height. This creates a homogenous sample of simultaneous AMVs, sondes and Profiler observations.

3. RESULTS

3.1. Rawinsonde to Wind Profiler Comparison

Figure 2 shows thecomparison between Wind Profiler and rawinsonde winds for the time period described above. There were 224790 matches for this comparison, yielding a directional RMS difference of 25.5°. The wind speed observations are essentially unbiased and have a speed RMS difference value of 2.2 ms^{-1}.

Figure 3 shows the height distribution of the sonde-Profiler matches. The vast majority of the matches are located in the upper troposphere, above the 500 hPa level. 50 of the 72 Wind Profiler sampling levels are above 500 hPa, which leads to the increased number of matches aloft. While a large number of matches were accumulated during the selected time period, and it appears that good agreement exists between these two datasets throughout the entire depth of the troposphere, it must be remembered that the sample is biased to

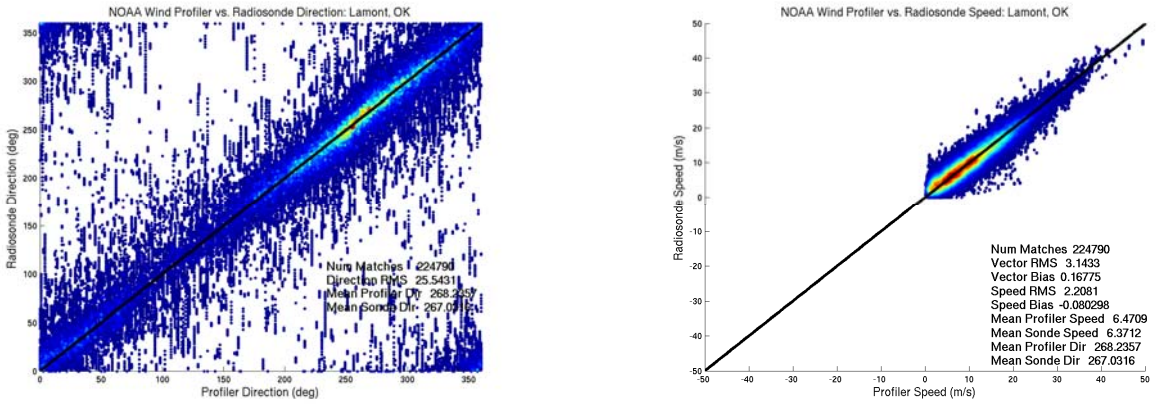

Figure 2: Collocated sonde and NOAA Wind Profiler wind direction (left) and wind speed (right) from 11 April to 1 October 2005 at Lamont, OK. RMS and bias statistics (degs and m/sec) are shown in the lower right.

lower wind speed regimes in the upper-troposphere due to the 25 km match radius constraint. It is likely that higher variability would exist in a 'climatologically-representative' sample. The poster presentation will explore this topic further, showing the difference characteristics for matches when the Wind Profiler is functioning in either "low" or "high" modes and when the observed winds are separated into speed intervals.

3.2. Mesoscale GOES-12 AMV Comparisons

A comparison between mesoscale GOES-12 AMVs, NOAA Wind Profiler, and rawinsonde wind observations is shown in Figure 4. For the 1847 matches shown here, the RMS difference statistics for both the AMV-Wind Profiler and AMV-rawinsonde comparisons are ~40° (~5.1 ms^{-1}) for wind direction (speed). Wind speed bias statistics reveal that the mesoscale AMVs are <1 ms^{-1} faster than the sonde and Profiler observations (see Table 1 at the end of the document). This finding is the reverse of usual AMV biases, as they have generally been found to be slower overall in comparison to sonde data in previous internal studies. We speculate that this "slow bias" in previous studies is caused by the inclusion of high wind regimes, which we are not sampling here due to the match radius and balloon drift limitation. Figure 5 shows that the matches are well distributed throughout the troposphere, with maximu matches in the lower troposphere (900-750 hPa) being mainly associated with VIS AMVs.

Table 1 provides a statistical comparison of mesoscale AMVs to sonde/Profiler, separated by AMV type and height. The parameter "Vector RMS" is defined as:

$$vect\_diff = \left(\sqrt{u\_diff^2 + v\_diff^2}\right)$$

$$vect\_RMS = \sqrt{\frac{\sum_{1}^{N}\left(vect\_diff\right)^2}{N}}$$

where *u_diff* and *v_diff* are the u- and v- wind component differences, *vect_diff* is the combined vector magnitude of *u_diff* and *v_diff*, and *N* is the total number of vectors in a given sample. "Vector Bias" is the mean *vect_diff* between the AMV and Profiler/sonde data.

Table 1 shows that AMVs within the lowest layer (1000-851 hPa) exhibit the highest directional RMS differences, as well as a reversal in speed bias compared to other layers. Vector biases are substantially higher for this layer than for the other three layers examined here, which is strongly influenced by the higher directional RMS differences. Higher directional RMS differences indicates that both the u- and v- wind components are significantly different, thus producing a higher mean vector difference (i.e. bias).

These results may be related to a couple issues. A high percentage of mesoscale AMVs from this layer are derived from VIS channel imagery. As the time period of this comparison falls within the "warm-season" over the U.S. Southern Plains, cloud "streets" composed of

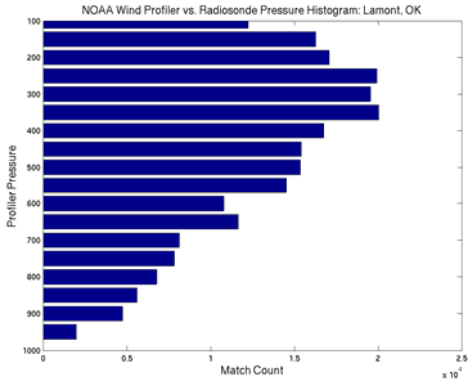

Figure 3: A histogram of the rawinsonde to NOAA Wind Profiler height matches for points shown in Fig. 2.

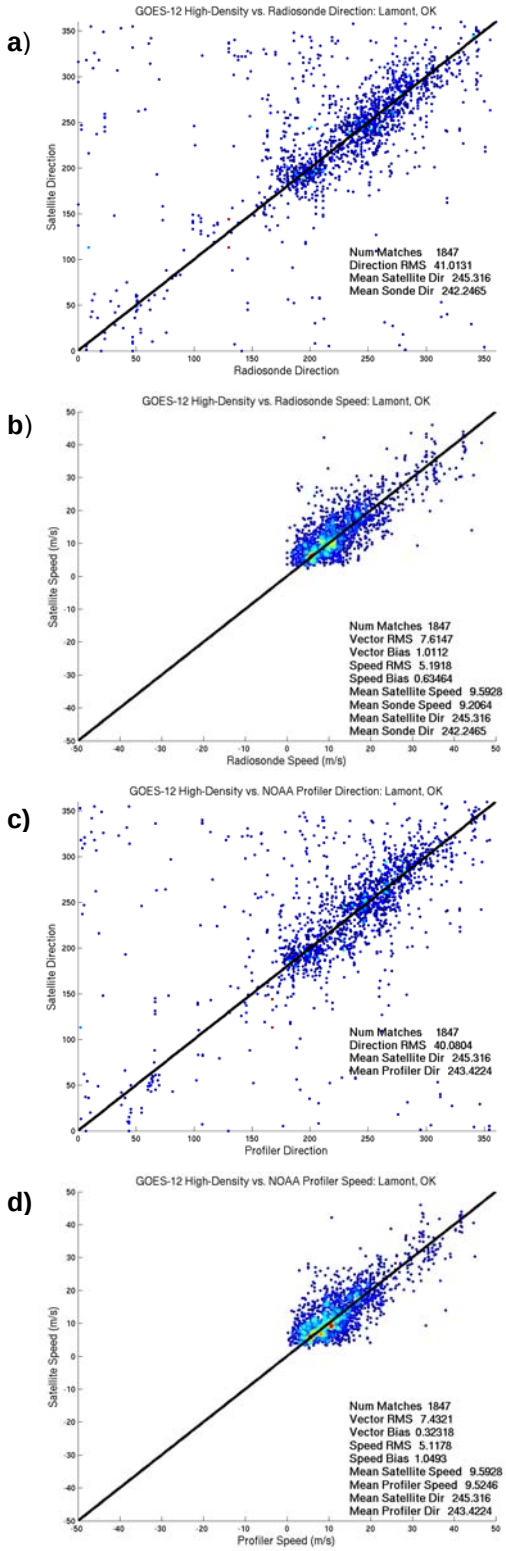

Figure 4: Collocated GOES-12 mesoscale AMV and rawinsonde (a) wind direction and (b) wind speed from 11 April to 1 October 2005 at Lamont, OK. (c-d) Same plots but for collocated AMV and NOAA Wind Profiler data. Warmer colors indicate higher scatterplot density.

small cumulus often form during the early afternoon and dissipate during the evening. These clouds appear very similar to one another within VIS imagery, making it more difficult for the correlation matching procedures to distinguish coherent cloud tracers. This may explain some of the larger differences in wind direction. Also, during the afternoon hours, strong solar insolation aids in the development of turbulent eddies within the convective boundary layer (CBL). These eddies draw higher momentum air downward, increasing the low-level wind speed. The Wind Profiler and sonde can observe this process, as they are measuring the flow from within the CBL, but the GOES satellite Imager does not have the needed vertical resolution, and this might be contributing to the negative bias in very low-level AMV speeds.

Another issue that may be leading to these results is related to limitations in VIS AMV height assignment accuracies for small (< 4-km width) cumulus clouds. VIS AMVs are generally assigned heights via the "IR window" technique, where the cloud-top 10.7-μm T_B is directly related to a NWP model temperature profile. When a VIS cloud feature does not fill an entire 4-km IR pixel, radiation from the earth's surface also reaches the satellite sensor, causing the IR T_B assigned to the VIS cloud to be warmer than its true cloud-top temperature. Thus, the cloud is assigned a height which is likely too low (Bedka et al. 2005), causing the AMV to be compared with flow from the wrong Profiler and sonde level. A small VIS cloud feature may be tracked perfectly in this case, but the resulting AMV could still carry an observation error as a result of this issue.

Table 1 also shows that WV and IR AMVs have higher RMS differences and biases than their VIS counterparts, but have smaller directional differences. It is important to note that, as IR and WV AMVs are primarily derived from upper-tropospheric features, they inherently observe flow of higher speed. Thus, WV and IR AMVs are more likely to possess higher RMS/bias values because they observe faster atmospheric flow. If the difference statistics are normalized by the mean vector speed within the set of matches for the 3 wind types, VIS (8.5 ms^{-1}), IR (12 ms^{-1}), and WV (16.5 ms^{-1}), VIS and WV vectors have nearly equivalent normalized

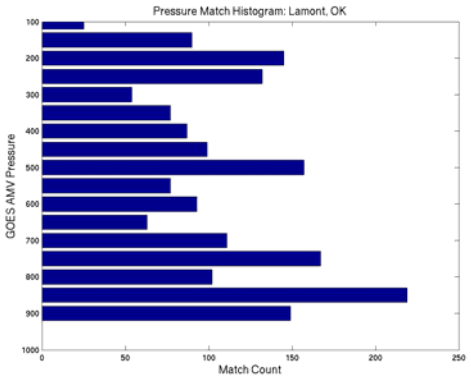

Figure 5: A histogram of the distribution of match heights for the points shown in Fig. 4. For reference, the bottom bar represents a height layer from 925 to 875 hPa.

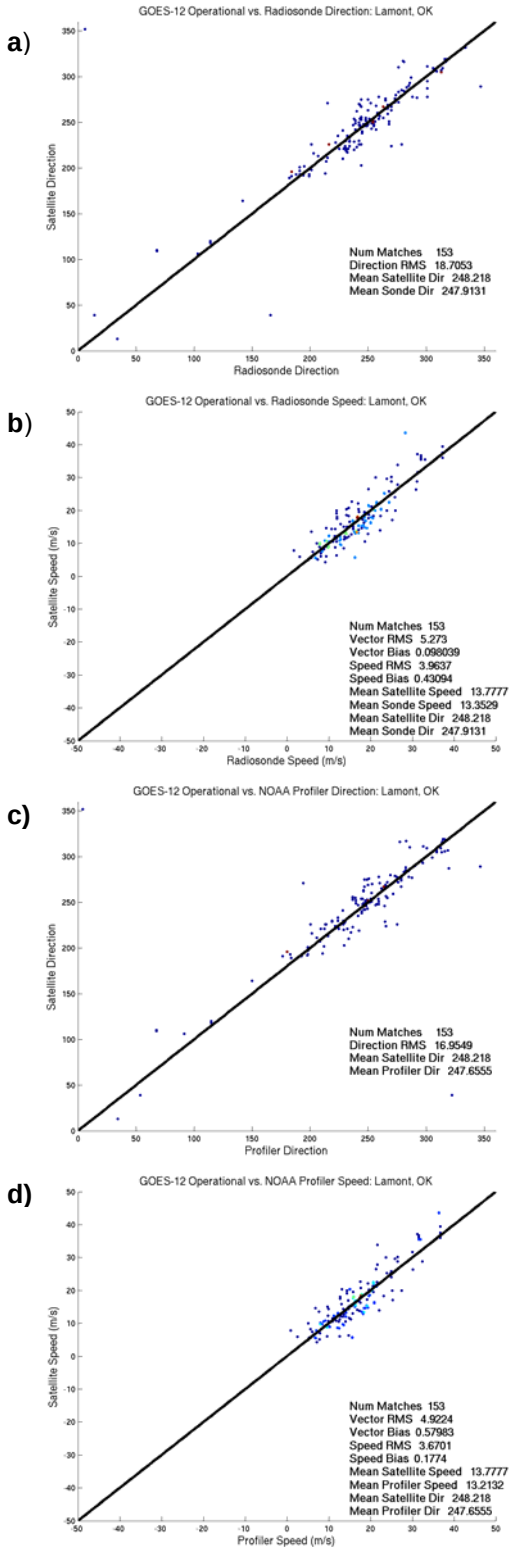

Figure 6: Collocated GOES operational AMV and rawinsonde (a) wind direction and (b) wind speed from 1 April to 1 October 2005 at Lamont, OK. (c-d) Same plots but for collocated AMV and NOAA Wind Profiler data. Warmer colors indicate higher scatterplot density.

differences, with the IR differences being slightly higher. WV directional differences are likely the smallest because upper-tropospheric flow is quite smooth, with the tracked WV gradients being consistent in magnitude and orientation within a 3-image (30 min) sequence. VIS and IR targets (clouds) can evolve more rapidly, leading to difficulties in estimating the "true" atmospheric flow from a satellite perspective.

3.3. Operational GOES-12 AMV Comparisons

Figure 6 is similar to Fig. 4 except that operational AMVs produced by NOAA/NESDIS (Nieman et al. 1997) are compared to the sonde and Profiler data. Only 153 data matches were present during the time frame of this study, compared to 1847 from the mesoscale AMV comparison. The operational AMVs have better agreement with the sonde/Profiler in both speed (~3.8 ms^{-1}) and direction (~17°) when compared to the difference statistics of the mesoscale AMVs. Operational vector speed biases are also smaller than those from the mesoscale vectors. These results are to be expected, as the operational AMV processing method incorporates a high degree of vector editing and quality control. These post-processing techniques provide more "accurate" wind estimates on average, but do not allow the operational AMVs to capture the level of detail contained within the mesoscale AMV fields (see BM05 for comparison of the two processing techniques). In addition, the bulk of the operational wind matches originate from the WV and IR channels, which appear to exhibit lower directional RMS characteristics based on the mesoscale AMV comparisons. Figure 7 shows that the vast majority of the operational AMVs are from the upper-troposphere, hence the average speed of the operational sample (13.8 ms^{-1}, not shown above) is higher than that of the mesoscale sample (9.6 ms^{-1}) used in this study.

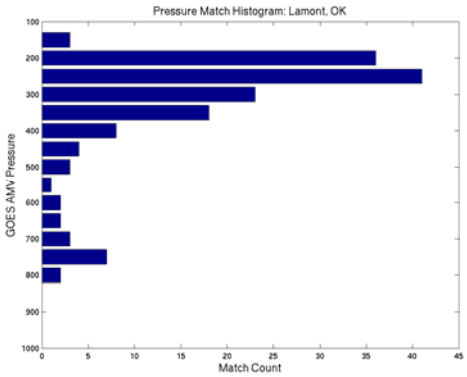

Figure 7: A histogram of the height distribution for the points shown in Fig. 6. The match count scale (x-axis) differs from that shown in Figure 5, as the total number of operational AMV matches is approx 10% of the mesoscale AMV matches. For reference, the bottom bar represents a height layer from 825 to 775 hPa.

Comparison Type	Number of Vectors	Direction RMS	Wind Speed Bias	Wind Speed RMS	Vector Bias	Vector RMS
AMV to Wind Profiler						
All Vectors	1847	40.08	1.05	5.12	.32	7.43
VIS/IR/WV 1000-851 hPa	225	55.91	-1.27	3.96	3.12	7.41
VIS/IR/WV 850-701 hPa	456	45.6	2.10	4.97	.07	7.29
VIS/IR/WV 700-400 hPa	593	33.36	.75	4.57	.23	6.89
VIS/IR/WV 400-100 hPa	573	32.33	1.42	6.10	.72	8.07
VIS only	1557	42.07	.85	4.49	.32	6.96
IR only	165	31.91	2.16	7.51	2.20	9.83
WV only	125	18.69	2.32	7.85	1.18	9.25
AMV to Rawinsonde						
All Vectors	1847	41.01	1.01	5.19	.63	7.61
VIS/IR/WV 1000-851 hPa	225	59.95	-.48	3.84	2.86	7.65
VIS/IR/WV 850-701 hPa	456	44.23	2.03	4.77	.87	6.99
VIS/IR/WV 700-400 hPa	593	34.79	.89	4.71	.41	7.04
VIS/IR/WV 400-100 hPa	573	33.19	.92	6.35	.54	8.57
VIS only	1557	42.65	.89	4.56	.50	7.05
IR only	165	36.09	1.64	7.83	1.98	10.44
WV only	125	22.09	1.86	7.66	1.26	9.73

Table 1: Mesoscale AMV comparisons to both Wind Profiler and rawinsonde, separated by AMV height and type. Positive speed and vector biases indicate that the GOES AMV is faster than the sonde or Profiler.

4. CONCLUSIONS

This study attempts to understand how well satellite AMVs can estimate the "true" wind, as measured by the NOAA Wind Profiler and rawinsonde at the ARM CART SGP Central Facility in Lamont, OK. Understanding the statistical difference characteristics between AMVs and actual flow measurements has strong implications for their use in aviation flight planning and safety applications, as well as in data assimilation. The first phase of this study shows that good agreement exists between the Wind Profiler and rawinsonde throughout the depth of the troposphere, thereby demonstrating the reliability of these data for use as "standards" in comparison to AMVs.

A direct comparison of mesoscale AMVs to these data shows RMS directional (speed) differences of ~40º (5.1 ms^{-1}) with a speed bias of 1 ms^{-1}. These differences may be attributed to a variety of factors such as errors in height assignment and problems in tracking evolving low level (1000-850 hPa) cumulus features in the VIS band during a U.S. Southern Plains summer. The collocated motion vectors are well distributed in the vertical with 84% of mesoscale AMV matches being derived from the VIS channel. The normalized VIS, IR, and WV AMV RMS statistics show that differences for the three channels are nearly equivalent when one accounts for the fact that higher wind speeds were sampled by IR and WV AMVs.

Mean operational NOAA/NESDIS operational directional (speed) RMS differences were found to be ~17º (3.8 ms^{-1}). The bulk of these matches were associated with IR and WV AMVs in the upper troposphere (above 400 hPa). 153 operational AMV matches were found here, representing only 8 % of the total mesoscale AMV match count. Data collection for this study will continue in time until a statistically significant operational AMV dataset is acquired, which will allow for a breakdown of statistics into AMV type and height.

5. ACKNOWLEDGEMENTS

The authors would like to thank Dave Stettner of the UW-CIMSS satellite winds group for providing the NOAA/NESDIS operational AMV data presented in this study and his collaboration in successfully implementing real-time mesoscale AMV processing. We also thank the U.S. Department of Energy as part of the Atmospheric Radiation Measurement Program Climate Research Facility for providing the rawinsonde profiles. This work is supported by the NASA Applied Sciences and the NASA Aviation Safety and Security Program through the NASA Advanced Satellite Aviation-weather Products (ASAP) subcontract #4400071484.

6. REFERENCES

Bedka, K. M. and J. R. Mecikalski, 2005: Application of satellite-derived atmospheric motion vectors for estimating mesoscale flows. *J. Appl. Meteor.*, *In press.*

Bedka, S. T., W. F. Feltz, A. J. Schreiner, and R.E. Holz, 2005: Satellite derived cloud top pressure product validation using aircraft based cloud physics lidar data from the AtREC field campaign. *International Journal of Remote Sensing. In press.*

Benjamin, S. G., J. M. Brown, K. J. Brundage, D. Devenyi, G. A. Grell, D. Kim, B. E. Schwartz, T. G. Smirnova, T. L. Smith, S. S. Weygandt, and G. S. Manikin, 2002: RUC20 - The 20-km version of the Rapid Update Cycle. NWS Technical Procedures Bulletin No. 490. [FSL revised version available through RUC web site at http://ruc.fsl.noaa.gov]

Hayden, C. M., and J. R. Purser, 1995: Recursive filter objective analysis of meteorological fields: Applications to NESDIS operational processing. *J. Appl. Meteor.*, **34**, 3-15.

Holmlund, K, 1998: The utilization of statistical properties of satellite-derived atmospheric motion vectors to derive quality indicators. *Wea. Forecasting,* **13**, 1093-1105.

Mecikalski, J. R., and K. M. Bedka, 2005: Forecasting convective initiation by monitoring the evolution of moving cumulus in daytime GOES imagery. *Mon. Wea. Rev., In press.*

Menzel, W. P., W. L. Smith, and T. R. Stewart, 1983: Improved cloud motion wind vector and altitude assignment using VAS. *J. Appl. Meteor*., **22**, 377-384.

Nieman, S. J., W. P. Menzel, C. M. Hayden, D. Gray, S. T. Wanzong, C. S. Velden, and J. Daniels, 1997: Fully automated cloud-drift winds in NESDIS operations. *Bull. Amer. Meteor. Soc.,* **78**, 1121-1133.

Rao, P. A., C. S. Velden, and S. A. Braun, 2002: The vertical error characteristics of GOES-derived winds: Description and experiments with numerical weather prediction. *J. Appl. Meteor*, **41**, 253–271.

Schreiner, A. J., D. A. Unger, W. P. Menzel, G. P. Ellrod, K. I. Strabala, and J. L. Pellett, 1993: A comparison of ground and satellite observations of cloud cover. *Bull. Amer. Meteor. Soc*., **74**, 1851-1861.

Szejwach, G., 1982: Determination of Semi-Transparent Cirrus Cloud Temperature from Infrared Radiance: Application to METEOSAT. *J. Appl. Meteor.,* **21**, 384–393.

Velden, C. S., C. M. Hayden, S. J. Nieman, W. P. Menzel, S. Wanzong, J. S. Goerss, 1997: Upper-tropospheric winds derived from geostationary satellite water vapor observations. *Bull. Amer. Meteor. Soc.*, **78**, 173-195.

Velden, C. S., T. L. Olander, and S. Wanzong, 1998: The impact of multispectral GOES-8 wind information on Atlantic tropical cyclone track forecasts in 1995. Part I: Dataset methodology, description, and case analysis. *Mon. Wea. Rev.*, **126**, 1202-1218.